This article has been accepted for publication in a future issue of this journal, but has not been fully edited. Content may change prior to final publication. Citation information: DOI 10.1109/TVT.2015.2416714, IEEE Transactions on Vehicular Technology

Uplink Achievable Rate and Power Allocation in Cooperative LTE-Advanced Networks

Xiaoxia Zhang, *Student Member, IEEE,* Xuemin (Sherman) Shen, *Fellow, IEEE,* and Liang-Liang Xie, *Senior Member, IEEE*

***Abstract*—This paper studies the achievable rate and power allocation to improve the uplink spectrum efficiency in an LTE-Advanced cooperative cellular network with the deployment of Type II in-band decode-and-forward relay stations (RSs). The physical layer uplink transmission technology is based on single carrier frequency division multiple access (SC-FDMA) with frequency-domain equalization (FDE). Different from the downlink orthogonal frequency division multiple access (OFDMA) system, signals on all subcarriers in the SC-FDMA system are transmitted sequentially rather than in parallel, thus the user's achievable rate is not simply the summation of the rates on all allocated subcarriers. Moreover, each user equipment (UE) has its own transmission power constraint instead of a total power constraint at the base station in the downlink case. Therefore, the uplink resource allocation problem in the LTE-Advanced system is more challenging. To this end, we first derive the achievable rates of the SC-FDMA system with two commonly-used FDE techniques, zero-forcing (ZF) equalization and minimum mean square error (MMSE) equalization, based on the joint superposition coding for cooperative relaying. We then propose optimal power allocation schemes among subcarriers at both UE and RS to maximize the overall throughput of the system. Both theoretical analysis and numerical results demonstrate that our proposed power allocation schemes can drastically improve the system throughput.**

***Index Terms*—Achievable rate, resource allocation, SC-FDMA, decode-and-forward relay, frequency-domain equalization, LTE-Advanced.**

I. Introduction

THE consumer demand for reliable high-speed communications has prompted the rapid evolution of mobile and cellular technologies over the past decades. Due to the emerging technologies and ever growing user and operator requirement, future-generation cellular systems are expected to further improve service provisioning at substantially reduced costs. In order to meet or exceed the International Mobile Telecommunications-Advanced (IMT-A) requirements, the Third Generation Partnership Project (3GPP) has launched the Long-Term Evolution (LTE) and its successor, LTE-Advanced (LTE-A) standard for cellular communications. The target is to support higher peak data rates, higher throughput and coverage, and lower latencies, resulting in a better user experience [1].

Xiaoxia Zhang, Xuemin (Sherman) Shen and Liang-Liang Xie are with the Department of Electrical and Computer Engineering, University of Waterloo, Waterloo, Ontario, Canada, N2L 3G1. E-mail: {x79zhang, sshen, llxie}@uwaterloo.ca.

To improve the spectrum efficiency and transmission rate, the physical layer techniques for LTE and LTE-A include orthogonal frequency division multiplexing (OFDM) as the downlink (DL) transmission scheme and SC-FDMA as the uplink (UL) multiple access scheme [2]. OFDM divides the bandwidth into subcarriers and allows flexible spectrum allocation to mitigate the time and frequency selective fading of wireless propagation channels. Although OFDM can substantially reduce the intersymbol interference (ISI) and increase the data rate, a principal weakness is the high peak-to-average power ratio (PAPR), which would impose a heavy burden on the power amplifier of the transmitter, especially for the mobile terminals [3]. As a result, SC-FDMA is proposed as the uplink transmission technique to reduce the PAPR and make the mobile terminals more power-efficient. SC-FDMA can be viewed as a discrete Fourier transform (DFT) precoded OFDMA, which is the multi-user version of OFDM. SC-FDMA can achieve similar throughput performance and overall complexity with OFDMA, yet reduce the PAPR and transmitter cost due to its inherent single carrier nature. Unlike OFDMA, both transmission and detection of the SC-FDMA signals are carried out in the time domain rather than in the frequency domain.

Besides the advanced physical layer transmission technologies, LTE-Advanced networks further incorporate several enhancements, e.g. carrier aggregation and heterogeneous network topologies to improve the capacity and coverage, and to ensure user fairness [1]. Among these, the introduction of relay stations (RSs) is of fundamental significance due to its capability of utilizing cooperative communications between the base stations/users and the relays [4]. There are mainly two types of relays supported by the LTE-Advanced standard. A Type I relay is a half-duplex relay deployed near the cell edge to extend the cellular coverage. It creates its own physical cell and appears as an eNodeB (eNB) or base station to all users within its transmission range. A Type II relay is a full-duplex relay which is transparent to all users. This type of relay is capable of cooperative communications and is deployed within a cell to increase the capacity of the users. With spatial separation, filtering, or enhanced interference cancellation, the full-duplex relays require no specific resource partitioning [5]. In terms of cooperation schemes, two most commonly studied in the literature are amplify-and-forward (AF) and decode-and-forward (DF) [6]. An AF relay simply amplifies the received signals and forwards them to the destination. Besides the desired signal, it also amplifies and propagates the interference and noise from the source-relay link. As the relay does

This article has been accepted for publication in a future issue of this journal, but has not been fully edited. Content may change prior to final publication. Citation information: DOI 10.1109/TVT.2015.2416714, IEEE Transactions on Vehicular Technology

not decode the message, the transmitted signal would cause interference to its own receiver as well. Therefore, extra resources such as frequency bands or time slots are needed at the AF relay for orthogonal transmission. On the other hand, DF relay could completely eliminate the noise since the relay decodes the received signal before forwarding, so the source and the relay are able to transmit on the same frequency band (channel) to improve the spectrum efficiency.

Considering the above physical layer techniques and relaying technologies, resource allocation for both downlink and uplink cellular networks has attracted an upsurge of research interest to utilize the limited spectral resources and to improve the network efficiency. Resource allocation in the traditional multiuser OFDMA downlink systems has been studied in numerous works, e.g. [7]–[10]. However, the optimality conditions and algorithms cannot be directly applied to the uplink case mainly for two reasons. Firstly, the capacity of the SC-FDMA system is not simply the summation of the capacity on each subcarriers as in OFDMA systems. Secondly, each UE has its own transmission power constraint instead of a total power constraint at the eNB in the downlink case. To this end, [11], [12] derived the single user transmission capacity of the SC-FDMA system with both ZF and MMSE equalization. [13] further designed low-complexity subcarrier and power allocation schemes to improve the communication reliability. Considering the unique features of the relay channels in the LTE-Advanced system, [14] studied the joint subcarrier, power and relay nodes allocation to maximize the transmission rate in the OFDMA system with AF relays. [15]–[17] proposed efficient resource allocation schemes for sum rate maximization for OFDMA system with DF relays.

For the uplink SC-FDMA system with relays, [6] studied joint source power allocation and AF relay beamforming in multi-relay networks to improve the energy efficiency. [18] calculated the signal-to-noise ratio (SNR) and proposed relay selection in an opportunistic AF relay-assisted SC-FDMA system and [19] studied relay selection and subcarrier allocation for opportunistic DF relay-aided SC-FDMA systems assuming that the UE cannot communicate with the eNB directly. However, to the best of our knowledge, there is limited literature on the capacity analysis and power allocation for the SC-FDMA system with cooperative decode-and-forward relays.

In this paper, we study the fundamental achievable rate and power allocation for the uplink communications in an LTE-Advanced network with the deployment of relay stations. We consider the in-band decode-and-forward (DF) Type II full-duplex relay since only this type of relay can achieve cooperative diversity gain by utilizing the broadcast nature of wireless channels. The in-band relay allocates the same set of frequency subcarriers for cooperative transmission with each UE. Upon receiving a signal from UE, the relay first decodes it to eliminate the noise, then retransmits to the eNB in its own codes. With joint superposition coding at the UE and the relay, higher rate can be achieved by improving the utilization of existing allocated spectral resources. The loop interference associated with full-duplex relays can be avoided by spatial isolation of the transmitting and receiving transceivers, and utilizing a loop interference suppression technique [20]. The main contributions of the paper include:

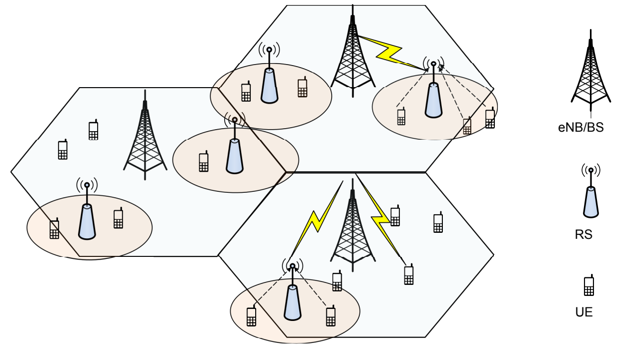

Fig. 1. Uplink transmission with the deployment of RSs in an LTE-Advanced network.

- Since SC-FDMA signals are no longer transmitted in parallel in the time domain, we revisit the joint superposition encoding and decoding processes for DF cooperative relaying in the frequency domain.
- We design ZF and MMSE equalizers at both RS and eNB taking into account the cooperative relay channels. Based on the proposed equalizers, the expressions of the achievable rate in the SC-FDMA relay system are derived.
- We propose optimal power allocation schemes among subcarriers at both UE and RS to maximize the overall throughput of the system.

The remainder of this paper is organized as follows. Section II introduces the uplink cooperative communications system model in an LTE-Advanced network. The transmitted and received signals at different nodes are shown in Section III. Section IV presents the joint superposition coding process and derives the expressions of the achievable rate of the uplink transmission with both ZF and MMSE equalization. Section V develops the power allocation schemes to maximize the throughput. The numerical results are included in Section VI and Section VII contains concluding remarks and possible future work.

II. System Model

The uplink cooperative communications framework in an LTE-Advanced network is shown in Fig. 1. In each cell, an eNB is located in the center where a set of UEs intend to connect to the eNB simultaneously for uplink transmission. Near the cell edge, several dedicated Type II in-band decode-and-forward relay stations are installed to assist the communications and improve the transmission rate for the users within the RS's communication range. We consider that the interference can be avoided by proper interference coordination among neighboring RSs, e.g., through careful carrier selection enabled by carrier aggregation in LTE-Advanced network. To simplify the problem, suppose no cooperation exists among adjacent RSs, so each user is served by at most one RS.

Each UE within the RS's coverage area broadcasts its transmission signals to both its affiliated eNB and the RS. The RS aids the communication in the sense that it first decodes the

This article has been accepted for publication in a future issue of this journal, but has not been fully edited. Content may change prior to final publication. Citation information: DOI 10.1109/TVT.2015.2416714, IEEE Transactions on Vehicular Technology

received signals from the UE, then forwards the message to the eNB in its own codes, which forms a three-node cooperative relay channel. Therefore, the eNB receives the superposition of the signals from two paths, the direct UE-eNB transmission link and the relay transmission link. Our discussion is limited to two-hop communications due to the drastic increase of the coding complexity associated with multiple hops [21].

The system model consists of one eNB, one RS and a set of M users, denoted by $\mathcal{M} = \{1, \ldots, M\}$, transmitting to the eNB with the help of the RS. The total available bandwidth B is divided into N orthogonal subcarriers indexed by $\mathcal{N} = \{1, \ldots, N\}$, where each subcarrier has a bandwidth of B/N. $\mathcal{N}_i \subset \mathcal{N}$ is the set of subcarriers occupied by user i for the uplink transmission. The number of subcarriers in $\mathcal{N}_i$ is denoted by N_i. Since LTE systems employ localized SC-FDMA as the uplink transmission technology, subcarriers assigned to a user need to be adjacent to each other [22]. Besides, each subcarrier can only be allocated to at most one user, i.e., $\mathcal{N}_i \bigcup \mathcal{N}_j = \emptyset,$ for $i, j \in \mathcal{M}, i \neq j$.

Consider that all wireless channels are independent and suffer from frequency selective fading and additive white Gaussian noise (AWGN). As the bandwidth of a single subcarrier is narrow, signals on each subcarrier experience frequency flat fading. The channel gain coefficients for user i, $i \in \mathcal{M}$ on subcarrier k, $k \in \mathcal{N}_i$ are denoted by $h_{s_i r}^{(k)}$, $h_{rd}^{(k)}$ and $h_{s_i d}^{(k)}$ representing the channel conditions of the UE-RS, RS-eNB and UE-eNB links, respectively. The corresponding frequency response are denoted by $H_{s_i r}^{(k)}$, $H_{rd}^{(k)}$ and $H_{s_i d}^{(k)}$. Based on the received pilot signals, we assume that RS has perfect knowledge of the channel state information (CSI) of the UE-RS link and eNB has the perfect knowledge of the CSI of all links in order to perform equalization and decoding. Based on the CSI, the resource scheduler located at the eNB allocates subcarriers and transmission power for both the UE and the RS before the uplink transmission. The decision is then fedback to the SC-FDMA transmitter scheduler at the UE and the RS for subcarrier mapping and power allocation.

III. Signal Representations in the SC-FDMA Relay System

The block diagram of the SC-FDMA transmitter and receiver structure for transmission of user i's signals is shown in Fig. 2.

SC-FDMA is also referred to as DFT-spread OFDMA. The sequence of the time-domain signals for transmission at user i is firstly transformed into frequency domain by the N_i-point DFT, then the sequence goes through the OFDMA processing. The decision is carried out in the time domain at the receiver after the N_i-point IDFT transforms the frequency-domain sequence into time domain.

A. Transmitted Signals at UE

The input to the transmitter at user i is a sequence of N_i time-domain symbols $\{x_{s_i}(u),\ u = 1, \ldots, N_i\}$. After the N_i-point DFT, it is transformed into a sequence of frequency-domain symbols $\{X_{s_i}(v),\ v = 1, \ldots, N_i\}$.

The frequency-domain scheduler then maps these symbols on a set of N_i active subcarriers selected from a total number of N subcarriers, and allocates the transmission power on each subcarrier. Assume the power allocated to subcarrier k for transmission at user i is $P_{s_i}^{(k)}$, which needs to satisfy a total power constraint:

$$\sum_{k \in \mathcal{N}_i} P_{s_i}^{(k)} \leq P_{s_i}, \tag{1}$$

where P_{s_i} is the total available transmission power at user i.

After the subcarrier mapping and power allocation, the frequency-domain signal on subcarrier k is denoted by $X_{s_i}^{(k)},\ k \in \mathcal{N}_i$. $X_{s_i}^{(k)}$ is then transformed back into time domain by the N-point inverse DFT (IDFT) before transmitting to the channel.

B. Received and Transmitted Signals at the RS

The sequence of the time-domain signals received at the RS is firstly transformed into the frequency domain by the N-point DFT. Denote $Y_r^{(k)},\ k \in \mathcal{N}_i$ as the frequency-domain representation of the received signal on subcarrier k at the RS, which is given by

$$Y_r^{(k)} = H_{s_i r}^{(k)} X_{s_i}^{(k)} + W_r^{(k)}, \tag{2}$$

where $W_r^{(k)}$ with variance σ_r^2 is the DFT of the additive white Gaussian noise received at the RS.

The frequency-domain equalization technique is utilized at the RS in order to mitigate the frequency selective fading effect induced by the wireless propagation channel. Then the sequence is transformed back to the time domain, denoted by $y_r(u),\ u = 1, \ldots, N_i$, for decoding, and the decoded message will be encoded and transmitted in the subsequent transmission block.

Upon receiving the signals from the users, the full-duplex RS transmits a sequence, $x_r(u),\ u = 1, \ldots, N_i$, to the SC-FDMA transmitter for cooperative transmission of user i's message. The same set of subcarriers $\mathcal{N}_i$ is selected at the RS for the transmission of user i's message. The frequency-domain representation of the transmitted signal on the kth subcarrier is $X_r^{(k)}, k \in \mathcal{N}_i$, and the power allocated to the k subcarrier is $P_r^{(k)}$, which satisfies:

$$\sum_{k \in \mathcal{N}} P_r^{(k)} \leq P_r, \tag{3}$$

where P_r is the total transmission power at the RS.

C. Received Signals at the eNB

The received signal at the eNB on subcarrier k is the superposition of the signal from the user and the signal from the RS, i.e.,

$$Y_d^{(k)} = H_{s_i d}^{(k)} X_{s_i}^{(k)} + H_{rd}^{(k)} X_r^{(k)} + W_d^{(k)}, \tag{4}$$

where $W_d^{(k)}$ is the additive white Gaussian noise received at the eNB on subcarrier k, and the variance is given by σ_d^2.

The corresponding time-domain symbols after the transformation for decision is denoted by the vector $y_d(u),\ u = 1, \ldots, N_i$.

This article has been accepted for publication in a future issue of this journal, but has not been fully edited. Content may change prior to final publication. Citation information: DOI 10.1109/TVT.2015.2416714, IEEE Transactions on Vehicular Technology

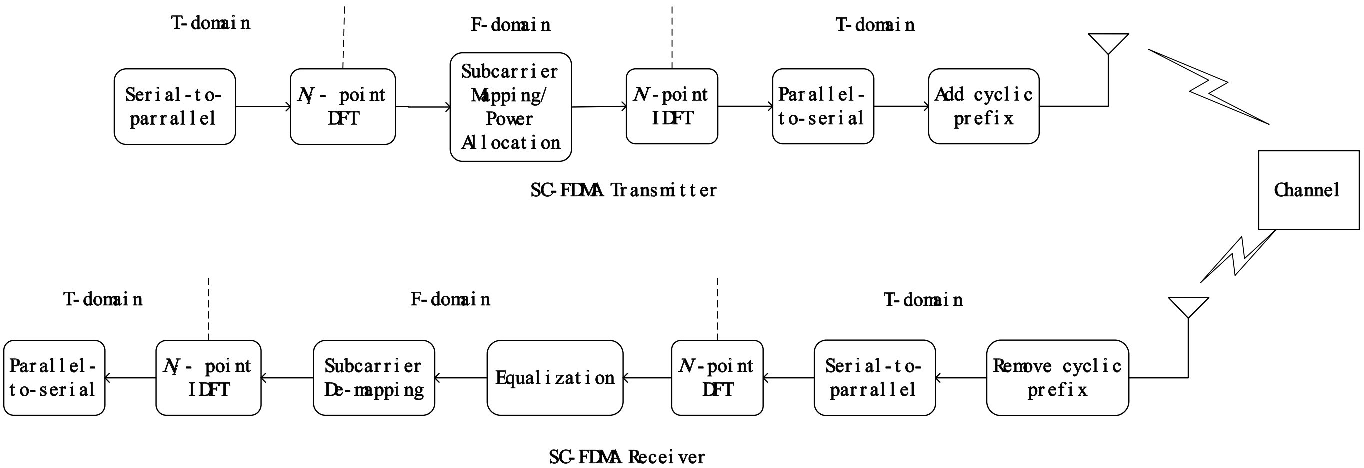

Fig. 2. SC-FDMA transmitter and receiver structure for transmission of user i's signals.

IV. Achievable Rates of the SC-FDMA Relay System

To avoid propagating noise and improve the transmission rate, the decode-and-forward RS cooperates with the UE to transmit the signals to the eNB. The achievable rate in the AWGN channel is attained by joint superposition coding which could maximize the cooperation between the source and the relay. The information theoretic achievable rate for the DF relay channel is given by [23]:

$$R = \max_{p(x_s, x_r)} \min\{I(X_s; Y_r|X_r), I(X_s, X_r; Y_d)\}. \quad (5)$$

The first term $I(X_s; Y_r|X_r)$ denotes the maximum rate for the relay to decode (relay decoding rate), and the second term $I(X_s, X_r; Y_d)$ represents the rate for the destination to successfully decode the message (destination decoding rate).

In this section, we consider the joint superposition coding with equalization techniques in the SC-FDMA system and derive the expressions of the achievable rate for ZF and MMSE equalization, respectively.

A. Joint Encoding

The joint superposition encoding process of the relay channel consists of a consecutive B blocks of transmission, indexed by $b = 1, \ldots, B$. During block b, a message w_b is transmitted over the channel. In each transmission block, two independent code words, $\boldsymbol{x_0}$ and $\boldsymbol{x_1}$, are employed, both of which contain N_i i.i.d. random variables generated according to normal distribution. $\boldsymbol{x_0}$ represents the current transmission block's message w_b while $\boldsymbol{x_1}$ includes the previous block's message w_{b-1}. RS transmits $\boldsymbol{x_1}$ with its full transmission power while UE transmits a superposition of $\boldsymbol{x_0}$ and $\boldsymbol{x_1}$ to achieve the cooperation, i.e.,

$$\begin{aligned} \boldsymbol{x_{s_i}} &= \sqrt{\beta}\boldsymbol{x_0} + \sqrt{\bar{\beta}}\boldsymbol{x_1}, \\ \boldsymbol{x_r} &= \boldsymbol{x_1}, \end{aligned} \quad (6)$$

where $0 \le \beta \le 1$ is the power dividing parameter and $\bar{\beta} = 1 - \beta$.

After the transmitter transforms the codes into frequency domain and performs subcarrier mapping and power allocation, the symbols transmitted on the kth subcarrier at the UE and RS are given by

$$\begin{aligned} X_{s_i}^{(k)} &= \sqrt{P_{s_i}^{(k)}}(\sqrt{\beta}X_0^{(k)} + \sqrt{\bar{\beta}}X_1^{(k)}), \\ X_r^{(k)} &= \sqrt{P_r^{(k)}}X_1^{(k)}, \end{aligned} \quad (7)$$

where $X_0^{(k)}$ and $X_1^{(k)}$ are the frequency-domain representations of $\boldsymbol{x_0}$ and $\boldsymbol{x_1}$ on the kth subcarrier, respectively.

B. Decoding at the RS

At the end of each transmission block, the relay receives (in the frequency domain):

$$\begin{aligned} Y_r^{(k)} &= H_{s_ir}^{(k)}X_{s_i}^{(k)} + W_r^{(k)} \\ &= \sqrt{\beta P_{s_i}^{(k)}}H_{s_ir}^{(k)}X_0^{(k)} + \sqrt{\bar{\beta}P_{s_i}^{(k)}}H_{s_ir}^{(k)}X_1^{(k)} + W_r^{(k)}. \end{aligned} \quad (8)$$

To eliminate the intersymbol interference and achieve similar performance of OFDMA with the same overall complexity, frequency-domain equalization is performed before the signals are transformed and decoded in the time domain. ZF and MMSE are the two commonly used frequency-domain equalization techniques in the SC-FDMA system. ZF equalization can completely eliminate the ISI with a simple structure. However, it degrades the system performance due to noise enhancement. Superior performance can be achieved using the MMSE equalization [24], [25]. In the following, the achievable rate of the SC-FDMA relay system is derived for both ZF and MMSE equalization techniques.

1) ZF equalization: If zero-forcing equalization technique is employed at the receiver, the output signal of the equalizer on subcarrier k is given by

$$\begin{aligned}Z_r^{(k)} =&\frac{Y_r^{(k)}}{\sqrt{\beta P_{s_i}^{(k)}}H_{s_ir}^{(k)}}\\ =&X_0^{(k)}+\sqrt{\bar{\beta}/\beta}X_1^{(k)}+\frac{W_r^{(k)}}{\sqrt{\beta P_{s_i}^{(k)}}H_{s_ir}^{(k)}}.\end{aligned} \quad (9)$$

The decoding process is carried out in the time domain. After the subcarrier de-mapping and IDFT, the uth element of the time-domain sequence $\boldsymbol{z_r}$ is given by

$$z_r(u)=\frac{1}{\sqrt{N_i}}\sum_{k=1}^{N_i}Z_r^{(k)}e^{j2\pi ku/N_i}=x_0(u)+$$
$$\sqrt{\bar{\beta}/\beta}\cdot x_1(u)+\frac{1}{\sqrt{N_i}}\sum_k\frac{W_r^{(k)}}{\sqrt{\beta P_{s_i}^{(k)}}H_{s_ir}^{(k)}}e^{j2\pi ku/N_i}. \quad (10)$$

Since $\boldsymbol{x_1}$ is the RS's transmitted symbol in the current transmission block, at the end of the transmission block b, RS needs to decode $\boldsymbol{x_0}$ and w_b, where w_b will be re-encoded and transmitted in the subsequent transmission block by the RS. The maximum achievable rate for the RS to decode $\boldsymbol{x_0}$ is given by

$$\begin{aligned}R_r^{\text{ZF}} =&I(X_0;Z_r|X_1)\\ =&C\left(\Big(\frac{1}{N_i}\sum_k\frac{\sigma_r^2}{\beta P_{s_i}^{(k)}|H_{s_ir}^{(k)}|^2}\Big)^{-1}\right),\end{aligned} \quad (11)$$

where $C(x)=\log_2(1+x)$.

2) MMSE equalization: Unlike ZF equalization, MMSE equalization technique also suppresses noise, thus it can achieve higher transmission rate. The output of an MMSE equalizer on the kth subcarrier is given by

$$\begin{aligned}Z_r^{(k)} =&\frac{\sqrt{\beta P_{s_i}^{(k)}}H_{s_ir}^{(k)^*}}{\beta P_{s_i}^{(k)}|H_{s_ir}^{(k)}|^2+\sigma_r^2}Y_r^{(k)}\\ =&\frac{\beta P_{s_i}^{(k)}|H_{s_ir}^{(k)}|^2}{\beta P_{s_i}^{(k)}|H_{s_ir}^{(k)}|^2+\sigma_r^2}X_0^{(k)}+\frac{\sqrt{\beta\bar{\beta}}P_{s_i}^{(k)}|H_{s_ir}^{(k)}|^2}{\beta P_{s_i}^{(k)}|H_{s_ir}^{(k)}|^2+\sigma_r^2}X_1^{(k)}\\ &+\frac{\sqrt{\beta P_{s_i}^{(k)}}H_{s_ir}^{(k)^*}}{\beta P_{s_i}^{(k)}|H_{s_ir}^{(k)}|^2+\sigma_r^2}W_r^{(k)}.\end{aligned} \quad (12)$$

The uth element of the time-domain sequence $\boldsymbol{z_r}$ is given by

$$\begin{aligned}z_r(u)=&\frac{1}{\sqrt{N_i}}\sum_k\frac{\beta P_{s_i}^{(k)}|H_{s_ir}^{(k)}|^2}{\beta P_{s_i}^{(k)}|H_{s_ir}^{(k)}|^2+\sigma_r^2}X_0^{(k)}e^{j2\pi ku/N_i}\\ &+\frac{1}{\sqrt{N_i}}\sum_k\frac{\sqrt{\beta\bar{\beta}}P_{s_i}^{(k)}|H_{s_ir}^{(k)}|^2}{\beta P_{s_i}^{(k)}|H_{s_ir}^{(k)}|^2+\sigma_r^2}X_1^{(k)}e^{j2\pi ku/N_i}\\ &+\frac{1}{\sqrt{N_i}}\sum_k\frac{\sqrt{\beta P_{s_i}^{(k)}}H_{s_ir}^{(k)^*}}{\beta P_{s_i}^{(k)}|H_{s_ir}^{(k)}|^2+\sigma_r^2}W_r^{(k)}e^{j2\pi ku/N_i}.\end{aligned} \quad (13)$$

Let

$$\lambda=\frac{1}{N_i}\sum_k\frac{\beta P_{s_i}^{(k)}|H_{s_ir}^{(k)}|^2}{\beta P_{s_i}^{(k)}|H_{s_ir}^{(k)}|^2+\sigma_r^2}, \quad (14)$$

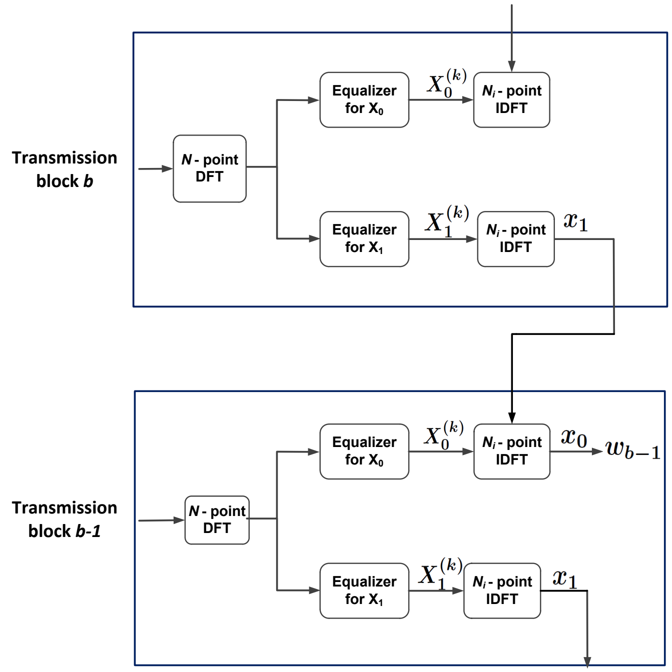

Fig. 3. Equalization and decoding process at the eNB.

the achievable rate to decode $\boldsymbol{x_0}$ with MMSE equalization is then given by

$$\begin{aligned}R_r^{\text{MMSE}} &= C\Big(\frac{\lambda^2}{\lambda-\lambda^2}\Big)\\ &=C\left(\frac{\frac{1}{N_i}\sum_k\frac{\beta P_{s_i}^{(k)}|H_{s_ir}^{(k)}|^2}{\beta P_{s_i}^{(k)}|H_{s_ir}^{(k)}|^2+\sigma_r^2}}{1-\frac{1}{N_i}\sum_k\frac{\beta P_{s_i}^{(k)}|H_{s_ir}^{(k)}|^2}{\beta P_{s_i}^{(k)}|H_{s_ir}^{(k)}|^2+\sigma_r^2}}\right)\\ &=C\left(\left[\Big(\frac{1}{N_i}\sum_k\frac{\beta P_{s_i}^{(k)}|H_{s_ir}^{(k)}|^2}{\beta P_{s_i}^{(k)}|H_{s_ir}^{(k)}|^2+\sigma_r^2}\Big)^{-1}-1\right]^{-1}\right).\end{aligned} \quad (15)$$

C. Decoding at the eNB

On the kth subcarrier, the destination eNB receives the superposition of the UE signal and the relay signal, i.e.,

$$\begin{aligned}Y_d^{(k)} &= H_{s_id}^{(k)}X_{s_i}^{(k)}+H_{rd}^{(k)}X_r^{(k)}+W_d^{(k)}\\ &=\sqrt{\beta P_{s_i}^{(k)}}H_{s_id}^{(k)}X_0^{(k)}+W_d^{(k)}+\\ &\left(\sqrt{\bar{\beta}P_{s_i}^{(k)}}H_{s_id}^{(k)}+\sqrt{P_r^{(k)}}H_{rd}^{(k)}\right)X_1^{(k)}.\end{aligned} \quad (16)$$

At the end of transmission block b, the eNB decodes the previous block's message w_{b-1} in two steps based on the received signals of both block b and $b-1$. Denote the time-domain symbol for decoding as z_d. First, $\boldsymbol{x_1}$ from block b is decoded at rate $R_{d1}=I(X_1;Z_d)$ while treating $\boldsymbol{x_0}$ as noise. Then based on the decoded $\boldsymbol{x_1}$, $\boldsymbol{x_0}$ from block $b-1$ and w_{b-1} are decoded at rate $R_d=I(X_0;Z_d|X_1)+R_{d1}=I(X_0,X_1;Z_d)$. The structure of the equalization and decoding process at the eNB in the SC-FDMA system is shown in Fig. 3.

At the end of each transmission block, the frequency-domain sequence after the N-point DFT goes into two parallel equalizers. The first equalizer is designed to equalize $X_1^{(k)}$ and the second equalizer is for $X_0^{(k)}$ equalization. Combined with the decoded $\boldsymbol{x_1}$ from block b, the joint decoding process in block $b-1$ is able to decode $\boldsymbol{x_0}$ and w_{b-1}.

1) ZF equalization: The kth element of the output signal of the ZF equalizer for $X_1^{(k)}$ can be written as the following frequency-domain representation:

$$\begin{aligned} Z_{d1}^{(k)} &= \frac{Y_d^{(k)}}{\sqrt{\bar{\beta}P_{s_i}^{(k)}}H_{s_id}^{(k)} + \sqrt{P_r^{(k)}}H_{rd}^{(k)}} \\ &= X_1^{(k)} + \frac{\sqrt{\beta P_{s_i}^{(k)}}H_{s_id}^{(k)}}{\sqrt{\bar{\beta}P_{s_i}^{(k)}}H_{s_id}^{(k)} + \sqrt{P_r^{(k)}}H_{rd}^{(k)}}X_0^{(k)} \\ &+ \frac{1}{\sqrt{\bar{\beta}P_{s_i}^{(k)}}H_{s_id}^{(k)} + \sqrt{P_r^{(k)}}H_{rd}^{(k)}}W_d^{(k)}. \end{aligned} \tag{17}$$

Then, the frequency-domain signal $Z_{d1}^{(k)}$ is transformed into time domain by IDFT. The uth element of the time-domain signal $\boldsymbol{z_{d1}}$ is given by

$$\begin{aligned} &z_{d1}(u) = x_1(u) \\ &+ \text{IDFT}\left(\frac{\sqrt{\beta P_{s_i}^{(k)}}H_{s_id}^{(k)}}{\sqrt{\bar{\beta}P_{s_i}^{(k)}}H_{s_id}^{(k)} + \sqrt{P_r^{(k)}}H_{rd}^{(k)}}X_0^{(k)}\right) \\ &+ \text{IDFT}\left(\frac{1}{\sqrt{\bar{\beta}P_{s_i}^{(k)}}H_{s_id}^{(k)} + \sqrt{P_r^{(k)}}H_{rd}^{(k)}}W_d^{(k)}\right). \end{aligned} \tag{18}$$

The maximum achievable rate for the eNB to decode $\boldsymbol{x_1}$ is given by

$$\begin{aligned} &R_{d1}^{\text{ZF}} = I(X_1; Z_{d1}) \\ &= C\left(\left(\frac{1}{N_i}\sum_k \frac{\beta P_{s_i}^{(k)}|H_{s_id}^{(k)}|^2 + \sigma_d^2}{\left|\sqrt{\bar{\beta}P_{s_i}^{(k)}}H_{s_id}^{(k)} + \sqrt{P_r^{(k)}}H_{rd}^{(k)}\right|^2}\right)^{-1}\right). \end{aligned} \tag{19}$$

Then, we decode $\boldsymbol{x_0}$ and the message w_{b-1}. The output signal of the equalizer for $X_0^{(k)}$ on the kth subcarrier can be calculated by

$$\begin{aligned} Z_{d2}^{(k)} &= \frac{Y_d^{(k)}}{\sqrt{\beta P_{s_i}^{(k)}}H_{s_id}^{(k)}} = X_0^{(k)} + \frac{1}{\sqrt{\beta P_{s_i}^{(k)}}H_{s_id}^{(k)}}W_d^{(k)} \\ &+ \frac{\sqrt{\bar{\beta}P_{s_i}^{(k)}}H_{s_id}^{(k)} + \sqrt{P_r^{(k)}}H_{rd}^{(k)}}{\sqrt{\beta P_{s_i}^{(k)}}H_{s_id}^{(k)}}X_1^{(k)}. \end{aligned} \tag{20}$$

The uth element of the time-domain signal after the IDFT can be written as

$$\begin{aligned} z_{d2}(u) &= x_0(u) + \text{IDFT}\left(\frac{1}{\sqrt{\beta P_{s_i}^{(k)}}H_{s_id}^{(k)}}W_d^{(k)}\right) \\ &+ \text{IDFT}\left(\frac{\sqrt{\bar{\beta}P_{s_i}^{(k)}}H_{s_id}^{(k)} + \sqrt{P_r^{(k)}}H_{rd}^{(k)}}{\sqrt{\beta P_{s_i}^{(k)}}H_{s_id}^{(k)}}X_1^{(k)}\right). \end{aligned} \tag{21}$$

Then, the total achievable rate for the destination to decode $\boldsymbol{x_0}$ and the previous block's message w_{b-1} with ZF equalization is given by

$$\begin{aligned} R_d^{\text{ZF}} &= I(X_0; Z_{d2}|X_1) + R_{d1}^{\text{ZF}} \\ &= C\left(\left(\frac{1}{N_i}\sum_k \frac{\sigma_d^2}{\beta P_{s_i}^{(k)}|H_{s_id}^{(k)}|^2}\right)^{-1}\right) + \\ &C\left(\left(\frac{1}{N_i}\sum_k \frac{\beta P_{s_i}^{(k)}|H_{s_id}^{(k)}|^2 + \sigma_d^2}{\left|\sqrt{\bar{\beta}P_{s_i}^{(k)}}H_{s_id}^{(k)} + \sqrt{P_r^{(k)}}H_{rd}^{(k)}\right|^2}\right)^{-1}\right). \end{aligned} \tag{22}$$

2) MMSE equalization: If MMSE equalization technique is employed at the receiver, the kth element of the output signal of the equalizer for $X_1^{(k)}$ in the frequency domain can be calculated by

$$\begin{aligned} Z_{d1}^{(k)} &= \frac{\left(\sqrt{\bar{\beta}P_{s_i}^{(k)}}H_{s_id}^{(k)} + \sqrt{P_r^{(k)}}H_{rd}^{(k)}\right)^*}{\left|\sqrt{\bar{\beta}P_{s_i}^{(k)}}H_{s_id}^{(k)} + \sqrt{P_r^{(k)}}H_{rd}^{(k)}\right|^2 + \sigma_d^2}Y_d^{(k)} \\ &= \frac{\left|\sqrt{\bar{\beta}P_{s_i}^{(k)}}H_{s_id}^{(k)} + \sqrt{P_r^{(k)}}H_{rd}^{(k)}\right|^2}{\left|\sqrt{\bar{\beta}P_{s_i}^{(k)}}H_{s_id}^{(k)} + \sqrt{P_r^{(k)}}H_{rd}^{(k)}\right|^2 + \sigma_d^2}X_1^{(k)} \\ &+ \frac{\sqrt{\beta P_{s_i}^{(k)}}H_{s_id}^{(k)}\left(\sqrt{\bar{\beta}P_{s_i}^{(k)}}H_{s_id}^{(k)} + \sqrt{P_r^{(k)}}H_{rd}^{(k)}\right)^*}{\left|\sqrt{\bar{\beta}P_{s_i}^{(k)}}H_{s_id}^{(k)} + \sqrt{P_r^{(k)}}H_{rd}^{(k)}\right|^2 + \sigma_d^2}X_0^{(k)} \\ &+ \frac{\left(\sqrt{\bar{\beta}P_{s_i}^{(k)}}H_{s_id}^{(k)} + \sqrt{P_r^{(k)}}H_{rd}^{(k)}\right)^*}{\left|\sqrt{\bar{\beta}P_{s_i}^{(k)}}H_{s_id}^{(k)} + \sqrt{P_r^{(k)}}H_{rd}^{(k)}\right|^2 + \sigma_d^2}W_d^{(k)}. \end{aligned} \tag{23}$$

The signal is then transformed into the time domain by the IDFT and the destination decodes the message based on the time-domain signal. Let

$$\lambda_1 = \frac{1}{N_i}\sum_k \frac{\left|\sqrt{\bar{\beta}P_{s_i}^{(k)}}H_{s_id}^{(k)} + \sqrt{P_r^{(k)}}H_{rd}^{(k)}\right|^2}{\left|\sqrt{\bar{\beta}P_{s_i}^{(k)}}H_{s_id}^{(k)} + \sqrt{P_r^{(k)}}H_{rd}^{(k)}\right|^2 + \sigma_d^2}. \tag{24}$$

The maximum achievable rate to decode $\boldsymbol{x_1}$ at the eNB is thus given by

$$\begin{aligned} &R_{d1}^{\text{MMSE}} = C\left(\frac{\lambda_1}{1-\lambda_1}\right) = \\ &C\left(\left[\left(\frac{1}{N_i}\sum_k \frac{\left|\sqrt{\bar{\beta}P_{s_i}^{(k)}}H_{s_id}^{(k)} + \sqrt{P_r^{(k)}}H_{rd}^{(k)}\right|^2}{\left|\sqrt{\bar{\beta}P_{s_i}^{(k)}}H_{s_id}^{(k)} + \sqrt{P_r^{(k)}}H_{rd}^{(k)}\right|^2 + \sigma_d^2}\right)^{-1} - 1\right]^{-1}\right). \end{aligned} \tag{25}$$

By the same argument, the kth element of the output signal of the MMSE equalizer for $X_0^{(k)}$ in the frequency domain is

This article has been accepted for publication in a future issue of this journal, but has not been fully edited. Content may change prior to final publication. Citation information: DOI 10.1109/TVT.2015.2416714, IEEE Transactions on Vehicular Technology

given by

$$Z_{d2}^{(k)} = \frac{\sqrt{\beta P_{s_i}^{(k)}} H_{s_i d}^{(k)^*}}{\beta P_{s_i}^{(k)} |H_{s_i d}^{(k)}|^2 + \sigma_d^2} Y_d^{(k)}$$
$$= \frac{\beta P_{s_i}^{(k)} |H_{s_i d}^{(k)}|^2}{\beta P_{s_i}^{(k)} |H_{s_i d}^{(k)}|^2 + \sigma_d^2} X_0^{(k)} + \frac{\sqrt{\beta P_{s_i}^{(k)}} H_{s_i d}^{(k)^*}}{\beta P_{s_i}^{(k)} |H_{s_i d}^{(k)}|^2 + \sigma_d^2} W_d^{(k)}$$
$$+ \frac{\sqrt{\beta P_{s_i}^{(k)}} H_{s_i d}^{(k)^*} \left(\sqrt{\bar{\beta} P_{s_i}^{(k)}} H_{s_i d}^{(k)} + \sqrt{P_r^{(k)}} H_{rd}^{(k)} \right)}{\beta P_{s_i}^{(k)} |H_{s_i d}^{(k)}|^2 + \sigma_d^2} X_1^{(k)}. \tag{26}$$

Denote λ_2 as

$$\lambda_2 = \frac{1}{N_i} \sum_k \frac{\beta P_{s_i}^{(k)} |H_{s_i d}^{(k)}|^2}{\beta P_{s_i}^{(k)} |H_{s_i d}^{(k)}|^2 + \sigma_d^2}. \tag{27}$$

Therefore, the maximum achievable rate for decoding $\boldsymbol{x_0}$ and w_{b-1} at the eNB with MMSE equalization can be calculated by

$$R_d^{\text{MMSE}} = C\left(\frac{\lambda_2}{1-\lambda_2}\right) + R_{d1}^{\text{MMSE}}$$
$$= C\left(\left[\left(\frac{1}{N_i} \sum_k \frac{\beta P_{s_i}^{(k)} |H_{s_i d}^{(k)}|^2}{\beta P_{s_i}^{(k)} |H_{s_i d}^{(k)}|^2 + \sigma_d^2} \right)^{-1} - 1 \right]^{-1} \right) +$$
$$C\left(\left[\left(\frac{1}{N_i} \sum_k \frac{\left| \sqrt{\bar{\beta} P_{s_i}^{(k)}} H_{s_i d}^{(k)} + \sqrt{P_r^{(k)}} H_{rd}^{(k)} \right|^2}{\left| \sqrt{\bar{\beta} P_{s_i}^{(k)}} H_{s_i d}^{(k)} + \sqrt{P_r^{(k)}} H_{rd}^{(k)} \right|^2 + \sigma_d^2} \right)^{-1} - 1 \right]^{-1} \right). \tag{28}$$

D. Achievable Rates

The maximum achievable rate for user i to transmit in the SC-FDMA system with the help of a relay station is the minimum of the RS decoding rate and the eNB decoding rate. If ZF equalization technique is utilized, the achievable rate for user i's transmission is given by

$$R_i^{\text{ZF}} = \max_{0<\beta<1} \min \left\{ R_r^{\text{ZF}}, R_d^{\text{ZF}} \right\}, \tag{29}$$

and the achievable rate with MMSE equalization technique is given by

$$R_i^{\text{MMSE}} = \max_{0<\beta<1} \min \left\{ R_r^{\text{MMSE}}, R_d^{\text{MMSE}} \right\}. \tag{30}$$

V. Power Allocation for Throughput Maximization

Based on the achievable rate of the SC-FDMA relay system derived in the previous section, we further allocate transmission power among the subcarriers at both UE and RS to maximize the cooperation gain and the overall throughput of the system.

The problem can be modeled mathematically as the following optimization problem:

$$\begin{aligned} \max_{P_{s_i}^{(k)}, P_r^{(k)}} \; & \sum_{i \in \mathcal{M}} R_i \\ \text{subject to} \; & \sum_{k \in \mathcal{N}_i} P_{s_i}^{(k)} \le P_{s_i}, \forall i \in \mathcal{M} \\ & \sum_{k \in \mathcal{N}} P_r^{(k)} \le P_r \\ & P_{s_i}^{(k)} \ge 0, \text{for all } k,\ i \\ & P_r^{(k)} \ge 0, \text{for all } k. \end{aligned} \tag{31}$$

The objective is to maximize the summation of the uplink achievable rates of all users in the network, where each user has its individual power constraint and the relay's transmission power on all subcarriers is bounded by a total power constraint.

Since (31) is a max-min problem, generally it is very difficult to solve. However, as each user occupies an exclusive set of subcarriers and has individual power constraint, this problem can be decomposed into a two-layer power allocation problem. Specifically, we first maximize the achievable rate of a single user through power allocation among its assigned subcarriers at both UE and RS assuming a fixed power constraint at the RS for the user, i.e.,

$$\begin{aligned} \max_{P_{s_i}^{(k)}, P_r^{(k)}} \; & R_i \\ \text{subject to} \; & \sum_{k \in \mathcal{N}_i} P_{s_i}^{(k)} \le P_{s_i} \\ & \sum_{k \in \mathcal{N}_i} P_r^{(k)} \le P_{r_i} \\ & P_{s_i}^{(k)} \ge 0, \text{for all } k \\ & P_r^{(k)} \ge 0, \text{for all } k. \end{aligned} \tag{32}$$

In (32), the total power available for relaying user i's information at the RS is denoted as P_{r_i}. In the second subproblem, the RS distributes its total available transmission power among all users to maximize the overall throughput, i.e.,

$$\begin{aligned} \max_{P_{r_i}} \; & \sum_{i \in \mathcal{M}} R_i \\ \text{subject to} \; & \sum_{i \in \mathcal{M}} P_{r_i} \le P_r \\ & P_{r_i} \ge 0, \text{for all } i. \end{aligned} \tag{33}$$

In the following, we consider the uplink SC-FDMA system employing ZF and MMSE equalization techniques and solve the two-layer optimization problem separately.

A. Power Allocation with ZF Equalization

The objective is to solve the two-layer optimization problem when a ZF equalization is utilized. In the uplink communication system, the transmission power and function at the transmitters are normally very limited. To simplify the transmitter design, we focus on the asynchronous relaying case with the power dividing parameter $\beta = 1$, i.e., the source and the relay use independent codes.

This article has been accepted for publication in a future issue of this journal, but has not been fully edited. Content may change prior to final publication. Citation information: DOI 10.1109/TVT.2015.2416714, IEEE Transactions on Vehicular Technology

In the asynchronous case, the single user's uplink achievable rate can be written as:

$$R_i^{\text{ZF}} = \min\Bigg\{ C\Bigg(\Big(\frac{1}{N_i}\sum_k \frac{\sigma_r^2}{P_{s_i}^{(k)}|H_{s_ir}^{(k)}|^2}\Big)^{-1}\Bigg), \\ C\Bigg(\Big(\frac{1}{N_i}\sum_k \frac{P_{s_i}^{(k)}|H_{s_id}^{(k)}|^2+\sigma_d^2}{P_r^{(k)}|H_{rd}^{(k)}|^2}\Big)^{-1}\Bigg)+ \\ C\Bigg(\Big(\frac{1}{N_i}\sum_k \frac{\sigma_d^2}{P_{s_i}^{(k)}|H_{s_id}^{(k)}|^2}\Big)^{-1}\Bigg)\Bigg\}, \quad (34)$$

where the first term denotes the relay decoding rate and the second term represents the eNB decoding rate.

Consider that in the uplink communications, the transmission power at the relay station is generally much greater than the available power at the mobile terminal, i.e., $P_r^{(k)} >> P_{s_i}^{(k)}$, which means that the relay decoding rate is the bottleneck of the achievable rate for user i. Since the relay decoding rate only depends on the allocated transmission power at the UE, (32) can be solved in two steps. First, we try to find the optimal power allocation among the assigned subcarriers at the UE to maximize the relay decoding rate, which is the upper bound of user i's achievable rate. Then, the optimal allocation of RS transmission power on each subcarrier can be determined to ensure that this upper bound is achievable.

Finding the optimal power allocation at the UE is equivalent to solving the following optimization problem:

$$\min_{P_{s_i}^{(k)}} \sum_{k\in\mathcal{N}_i} \frac{\sigma_r^2}{P_{s_i}^{(k)}|H_{s_ir}^{(k)}|^2} \\ \text{subject to} \sum_{k\in\mathcal{N}_i} P_{s_i}^{(k)} \le P_{s_i} \\ P_{s_i}^{(k)} \ge 0. \quad (35)$$

Since (35) is a convex optimization problem, the Kuhn-Tucker condition (KKT condition) characterizes the necessary and sufficient condition that the optimal solution needs to satisfy. The Lagrangian can be written as

$$\mathcal{L} = \sum_{k\in\mathcal{N}_i} \frac{\sigma_r^2}{P_{s_i}^{(k)}|H_{s_ir}^{(k)}|^2} + \lambda\Big(\sum_{k\in\mathcal{N}_i} P_{s_i}^{(k)} - P_{s_i}\Big), \quad (36)$$

and the KKT condition is given by

$$\frac{\partial\mathcal{L}}{\partial P_{s_i}^{(k)}} = \lambda - \frac{\sigma_r^2}{|H_{s_ir}^{(k)}|^2}\frac{1}{{P_{s_i}^{(k)}}^2} = 0, \quad (37)$$

where λ is chosen to satisfy the UE's transmission power constraint $\sum_{k\in\mathcal{N}_i} P_{s_i}^{(k)} \le P_{s_i}$.

Solving (37), the optimal $P_{s_i}^{(k)*}$ is given by

$$P_{s_i}^{(k)*} = \frac{P_{s_i}}{|H_{s_ir}^{(k)}| \cdot \sum_{k\in\mathcal{N}_i} |H_{s_ir}^{(k)}|^{-1}}. \quad (38)$$

Then, the optimal $P_r^{(k)*}$ should maximize the eNB decoding rate with $P_{s_i}^{(k)*}$ given in (38). Specifically, $P_r^{(k)*}$ can be obtained by the KKT condition with the following Lagrangian:

$$\mathcal{L} = \sum_{k\in\mathcal{N}_i} \frac{P_{s_i}^{(k)}|H_{s_id}^{(k)}|^2+\sigma_d^2}{P_r^{(k)}|H_{rd}^{(k)}|^2} + \mu\Big(\sum_{k\in\mathcal{N}_i} P_r^{(k)} - P_{r_i}\Big). \quad (39)$$

The KKT condition is given by

$$\frac{\partial\mathcal{L}}{\partial P_r^{(k)}} = \mu - \frac{P_{s_i}^{(k)}|H_{s_id}^{(k)}|^2+\sigma_d^2}{P_r^{(k)}|H_{rd}^{(k)}|^2} \cdot \frac{1}{{P_r^{(k)}}^2} = 0, \quad (40)$$

where μ is chosen to satisfy the RS power constraint $\sum_{k\in\mathcal{N}_i} P_r^{(k)} \le P_{r_i}$.

Solving (40), the optimal $P_r^{(k)*}$ is given by

$$P_r^{(k)*} = \frac{P_{r_i}}{\sum_{k\in\mathcal{N}_i} \frac{\sqrt{P_{s_i}^{(k)*}|H_{s_id}^{(k)}|^2+\sigma_d^2}}{|H_{rd}^{(k)}|}} \cdot \frac{\sqrt{P_{s_i}^{(k)*}|H_{s_id}^{(k)}|^2+\sigma_d^2}}{|H_{rd}^{(k)}|}. \quad (41)$$

To solve subproblem (33), we need to allocate the RS transmission power among users to maximize the overall throughput of the system. Consider that the available transmission power at the RS is sufficient enough compared with the total power at the UE, and the eNB decoding rate increases with P_{r_i} while the RS decoding rate remains unchanged. The optimal $P_{r_i}^*$ is the smallest value that can make the eNB decoding rate equal the RS decoding rate, thus the upper bound of each user's achievable rate can be achieved. Therefore, the optimal RS transmission power for relaying user i's information $P_{r_i}^*$ can be attained by solving the following equation:

$$C\Bigg(\Big(\frac{1}{N_i}\sum_k \frac{P_{s_i}^{(k)*}|H_{s_id}^{(k)}|^2+\sigma_d^2}{P_r^{(k)*}|H_{rd}^{(k)}|^2}\Big)^{-1}\Bigg) \\ = C\Bigg(\Big(\frac{1}{N_i}\sum_k \frac{\sigma_r^2}{P_{s_i}^{(k)*}|H_{s_ir}^{(k)}|^2}\Big)^{-1}\Bigg) - \\ C\Bigg(\Big(\frac{1}{N_i}\sum_k \frac{\sigma_d^2}{P_{s_i}^{(k)*}|H_{s_id}^{(k)}|^2}\Big)^{-1}\Bigg). \quad (42)$$

B. Power Allocation with MMSE Equalization

The single user's achievable rate in the asynchronous relaying case when MMSE equalization technique is employed is given by

$$R_i^{\text{MMSE}} = \\ \min\Bigg\{ C\Bigg(\Big[\Big(\frac{1}{N_i}\sum_k \frac{P_{s_i}^{(k)}|H_{s_ir}^{(k)}|^2}{P_{s_i}^{(k)}|H_{s_ir}^{(k)}|^2+\sigma_r^2}\Big)^{-1} - 1\Big]^{-1}\Bigg), \\ C\Bigg(\Big[\Big(\frac{1}{N_i}\sum_k \frac{P_r^{(k)}|H_{rd}^{(k)}|^2}{P_r^{(k)}|H_{rd}^{(k)}|^2+\sigma_d^2}\Big)^{-1} - 1\Big]^{-1}\Bigg)+ \\ C\Bigg(\Big[\Big(\frac{1}{N_i}\sum_k \frac{P_{s_i}^{(k)}|H_{s_id}^{(k)}|^2}{P_{s_i}^{(k)}|H_{s_id}^{(k)}|^2+\sigma_d^2}\Big)^{-1} - 1\Big]^{-1}\Bigg)\Bigg\}. \quad (43)$$

When $P_r^{(k)} >> P_{s_i}^{(k)}$, the relay decoding rate is the bottleneck of (43). To find the optimal user transmission power allocation to maximize the relay decoding rate, we first solve

This article has been accepted for publication in a future issue of this journal, but has not been fully edited. Content may change prior to final publication. Citation information: DOI 10.1109/TVT.2015.2416714, IEEE Transactions on Vehicular Technology

the following optimization problem:

$$\begin{aligned} \max_{P_{s_i}^{(k)}} & \sum_{k\in\mathcal{N}_i} \frac{P_{s_i}^{(k)}|H_{s_ir}^{(k)}|^2}{P_{s_i}^{(k)}|H_{s_ir}^{(k)}|^2+\sigma_r^2} \\ \text{subject to} & \sum_{k\in\mathcal{N}_i} P_{s_i}^{(k)} \le P_{s_i} \\ & P_{s_i}^{(k)} \ge 0. \end{aligned} \tag{44}$$

(44) is also a convex optimization problem where the Lagrangian is given by

$$\mathcal{L}=\sum_{k\in\mathcal{N}_i} \frac{P_{s_i}^{(k)}|H_{s_ir}^{(k)}|^2}{P_{s_i}^{(k)}|H_{s_ir}^{(k)}|^2+\sigma_r^2} - \lambda\Big(\sum_{k\in\mathcal{N}_i} P_{s_i}^{(k)} - P_{s_i}\Big), \tag{45}$$

and the KKT condition is given by

$$\frac{\partial\mathcal{L}}{\partial P_{s_i}^{(k)}} = \frac{|H_{s_ir}^{(k)}|^2\sigma_r^2}{\left(P_{s_i}^{(k)}|H_{s_ir}^{(k)}|^2+\sigma_r^2\right)^2} - \lambda = 0, \tag{46}$$

where λ is determined by the transmission power constraint at user i, i.e., $\sum_{k\in\mathcal{N}_i} P_{s_i}^{(k)} \le P_{s_i}$.

Hence the optimal $P_{s_i}^{(k)*}$ is a water-filling solution given by

$$P_{s_i}^{(k)*} = \left(\frac{\sigma_r}{|H_{s_ir}^{(k)}|\sqrt{\lambda}} - \frac{\sigma_r^2}{|H_{s_ir}^{(k)}|^2}\right)^+, \tag{47}$$

where function $(\cdot)^+$ is defined as

$$(x)^+ = \begin{cases} x, & \text{if } x \ge 0; \\ 0, & \text{if } x < 0. \end{cases} \tag{48}$$

The optimal power allocated to subcarrier k at the RS, $P_r^{(k)*}$, needs to maximize the eNB decoding rate with $P_{s_i}^{(k)*}$ given in (47). The Lagrangian is given by

$$\mathcal{L}=\sum_{k\in\mathcal{N}_i} \frac{P_r^{(k)}|H_{rd}^{(k)}|^2}{P_r^{(k)}|H_{rd}^{(k)}|^2+\sigma_d^2} - \mu\Big(\sum_{k\in\mathcal{N}_i} P_r^{(k)} - P_{r_i}\Big), \tag{49}$$

and the KKT condition can be written as

$$\frac{\partial\mathcal{L}}{\partial P_r^{(k)}} = \frac{|H_{rd}^{(k)}|^2\sigma_d^2}{\left(P_r^{(k)}|H_{rd}^{(k)}|^2+\sigma_d^2\right)^2} - \mu = 0, \tag{50}$$

where μ is chosen to satisfy the transmission power constraint at the RS, i.e., $\sum_{k\in\mathcal{N}_i} P_r^{(k)} \le P_{r_i}$.

The optimal $P_r^{(k)*}$ is also a water-filling solution given by

$$P_r^{(k)*} = \left(\frac{\sigma_d}{|H_{rd}^{(k)}|\sqrt{\mu}} - \frac{\sigma_d^2}{|H_{rd}^{(k)}|^2}\right)^+. \tag{51}$$

To maximize the overall throughput of the system, the optimal RS transmission power allocated for relaying user i's message, $P_{r_i}^*$, is the smallest value that can achieve the upper bound of user i's achievable rate. Specifically, $P_{r_i}^*$ makes the user i's RS decoding rate equal the eNB decoding rate and thus can be obtained by solving the following equation:

$$\begin{aligned} &C\left(\left[\Big(\frac{1}{N_i}\sum_k \frac{P_r^{(k)*}|H_{rd}^{(k)}|^2}{P_r^{(k)*}|H_{rd}^{(k)}|^2+\sigma_d^2}\Big)^{-1} - 1\right]^{-1}\right) \\ =&C\left(\left[\Big(\frac{1}{N_i}\sum_k \frac{P_{s_i}^{(k)*}|H_{s_ir}^{(k)}|^2}{P_{s_i}^{(k)*}|H_{s_ir}^{(k)}|^2+\sigma_r^2}\Big)^{-1} - 1\right]^{-1}\right) - \\ &C\left(\left[\Big(\frac{1}{N_i}\sum_k \frac{P_{s_i}^{(k)*}|H_{s_id}^{(k)}|^2}{P_{s_i}^{(k)*}|H_{s_id}^{(k)}|^2+\sigma_d^2}\Big)^{-1} - 1\right]^{-1}\right). \end{aligned} \tag{52}$$

VI. Numerical Results

To verify the derived uplink achievable rates and evaluate the performance of the proposed power allocation schemes in SC-FDMA relay systems, in this section, we present our numerical results considering practical network scenarios.

We consider that all wireless channels suffer from independent frequency selective fading and each subcarrier is subject to frequency flat Rayleigh fading. In our simulation, a typical urban area propagation model with 9 paths is employed [26], and the parameters are listed in Table I.

TABLE I
Relative powers of the delay profile.

Delay (μs)	0.0	0.05	0.12	0.2	0.23	0.5	1.6	2.3	5.0
Power (dB)	-1.0	-1.0	-1.0	0.0	0.0	0.0	-3.0	-5.0	-7.0

Fig. 4 shows the RS decoding rate and the eNB decoding rate with different power dividing parameter β for both ZF equalization and MMSE equalization in a single user SC-FDMA system. The uplink user equipment is allocated with one resource block, i.e., 12 consecutive subcarriers for transmission. The transmission power is 15dBm at both UE and RS, and is equally assigned to all allocated subcarriers. The noise variance received at the RS on each subcarrier is normalized to 1, and the noise variance at the eNB is 2. It can be seen that MMSE equalization generally achieves higher rate than ZF equalization due to noise suppression. The user's achievable rate is the minimum of its RS decoding rate and eNB decoding rate. The maximum user's achievable rate is achieved with the

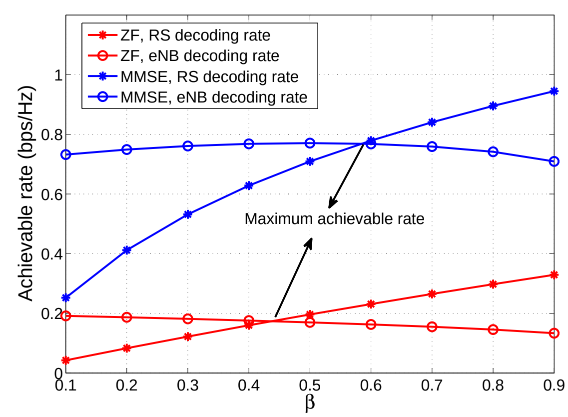

Fig. 4. RS decoding rate and eNB decoding rate with ZF and MMSE equalization.

This article has been accepted for publication in a future issue of this journal, but has not been fully edited. Content may change prior to final publication. Citation information: DOI 10.1109/TVT.2015.2416714, IEEE Transactions on Vehicular Technology

optimal power dividing parameter which ensures that the user's RS decoding rate equals its eNB decoding rate.

Fig. 5 shows the maximum achievable rate of a single user in both OFDMA and SC-FDMA systems with MMSE and ZF equalization techniques. We compare the derived achievable rate of the decode-and-forward relay channel with the single user's capacity of the direct transmission without the help of RSs. The user's achievable rate of the relay channel in the OFDMA network is calculated based on equation (4) in [16]. The capacity of the SC-FDMA system is determined according to equation (9) and (12) for ZF equalization and MMSE equalization, respectively. The total transmission power at the UE and RS ranges from 20dBm to 30dBm for the relaying case while the UE power matches the total transmission power for the direct transmission case in order to conduct a fair comparison. The transmission power is equally distributed on all subcarriers in both cases. The rest of the simulation parameters remain unchanged.

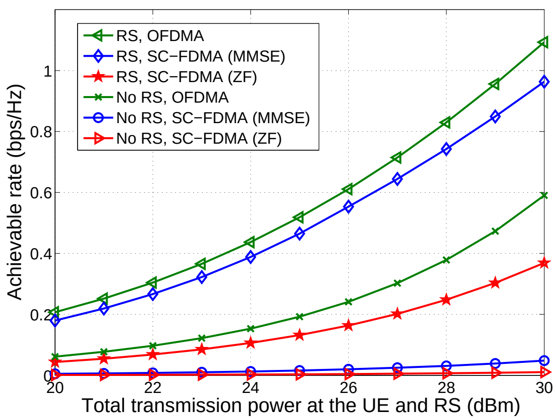

Fig. 5. Rate comparison of SC-FDMA and OFDMA relay systems.

In Fig. 5, it can be seen that the spectrum efficiency of both SC-FDMA and OFDMA systems with and without relay stations increases with the total transmission power. In wireless environment, OFDMA achieves higher rate than SC-FDMA due to the parallel transmission structure of OFDMA signals. Fig. 5 also shows that the cooperative transmission with the help of a decode-and-forward relay can significantly improve the user rate compared with non-cooperative transmission, which demonstrates the benefits of deploying relay stations in the cellular network.

To evaluate the performance of our proposed power allocation schemes for both ZF and MMSE equalization, we first compare the single user's achievable rate achieved by our proposed power allocation schemes with an equal power allocation scheme, which is most commonly employed for deriving capacity and resource allocation schemes [11], [12] as shown in Fig. 6. The equal power allocation scheme assigns the transmission power at both UE and RS equally to all subcarriers. Consider that the transmission power at the UE is 25dBm and the transmission power at the RS for each user is fixed and ranges from 30dBm to 45dBm.

It can be seen that our proposed power allocation schemes

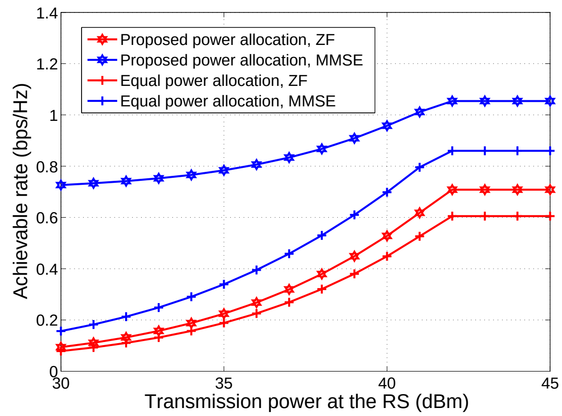

Fig. 6. Comparison of single-user uplink achievable rates.

can improve the single user's achievable rate for both ZF and MMSE equalization compared with the equal power allocation scheme. As the RS's transmission power increases, the eNB decoding rate rises accordingly while the RS decoding rate remains unchanged. Thus, the single user's achievable rate reaches an upper bound, which is determined by the RS decoding rate.

Fig. 7 compares the overall throughput of our proposed power allocation schemes and the equal power allocation scheme in the uplink transmission of a cellular network. The RS's total available transmission power is 50dBm, which is allocated among all users according to (42) and (52). Some simulation parameters are summarized in Table II:

TABLE II
SIMULATION PARAMETERS.

Parameter	Value
Cellular layout	Hexagonal grid, 6 sectors per cell
Relay station layout	1 relay station per sector
Relay protocol	Decode-and-Forward
Transmission bandwidth	20MHz
Subcarrier separation	15kHz
♯ of subcarriers in a resource block	12
Carrier frequency	2GHz for uplink
Channel model	Frequency selective Rayleigh fading
UE distribution	Uniformly random
UE transmission power	25dBm
RS transmission power	50dBm

Since each user occupies only one resource block, the uplink transmission bandwidth is sufficient. Therefore, it can be seen that both throughput achieved by our proposed power allocation schemes and the throughput achieved by equal power allocation scheme increase with the number of users. Furthermore, our proposed power allocation schemes outperform the equal power allocation scheme drastically, especially in the MMSE equalization scenario. The ZF equalization shows a poor noise performance and the improvement is relatively limited as the noise contributions of highly attenuated subchannels are rather large, which limit the overall system performance.

VII. CONCLUSION

In this paper, we have studied the cooperative transmission and power allocation to improve the transmission efficiency in

This article has been accepted for publication in a future issue of this journal, but has not been fully edited. Content may change prior to final publication. Citation information: DOI 10.1109/TVT.2015.2416714, IEEE Transactions on Vehicular Technology

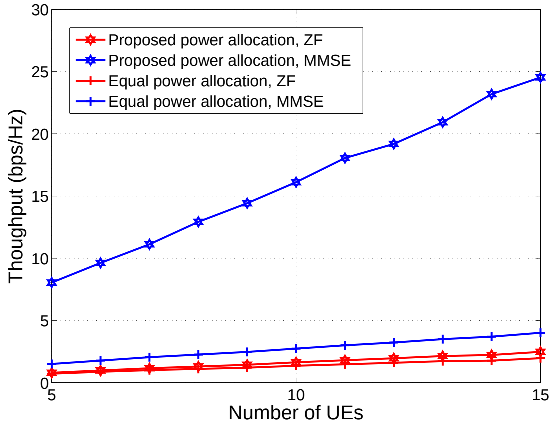

Fig. 7. Comparison of the overall throughput in an uplink cellular network.

an uplink LTE-Advanced cellular system with Type II in-band decode-and-forward relays. As SC-FDMA is the physical layer technique for the LTE-Advanced system, the capacity and resource allocation schemes for the downlink OFDMA system cannot be applied directly to the SC-FDMA system. Therefore, we have first studied the joint superposition coding and derived the expressions of the achievable rate of an uplink SC-FDMA relay system with both ZF and MMSE equalization. Then we have proposed optimal power allocation schemes to maximize the overall throughput of the system.

For the future work, we will jointly consider subcarrier and power allocation, and propose efficient resource allocation algorithms for practical uplink communication scenarios to further improve the spectrum efficiency.

REFERENCES

[1] A. Ghosh, R. Ratasuk, B. Mondal, N. Mangalvedhe, and T. Thomas, “LTE-Advanced: next-generation wireless broadband technology,” *IEEE Transactions on Wireless Communications*, vol. 17, no. 3, pp. 10–22, 2010.

[2] 3GPP. TS 36.201 Technical Specification Group Radio Access Network; Evolved Universal Terrestrial Radio Access (E-UTRA); Long Term Evolution (LTE) Physical Layer; General Description (Release 8).

[3] H. G. Myung and D. Goodman, *Single Carrier FDMA: a new air interface for long term evolution*. John Wiley & Sons, 2008.

[4] E. Altubaishi and X. Shen, “Performance analysis of spectrally efficient amplify-and-forward opportunistic relaying scheme for adaptive cooperative wireless systems,” *Wireless Communications and Mobile Computing (Wiley)*, July 2013.

[5] P. Bhat, S. Nagata, L. Campoy, I. Berberana, T. Derham, G. Liu, X. Shen, P. Zong, and J. Yang, “LTE-Advanced: an operator perspective,” *IEEE Communications Magazine*, vol. 50, no. 2, pp. 104–114, 2012.

[6] H. Kha, H. Tuan, and H. Nguyen, “Joint optimization of source power allocation and cooperative beamforming for SC-FDMA multi-user multi-relay networks,” *IEEE Transactions on Communications*, vol. 61, no. 6, pp. 2248–2259, 2013.

[7] X. Wang and G. B. Giannakis, “Resource allocation for wireless multiuser OFDM networks,” *IEEE Transactions on Information Theory*, vol. 57, no. 7, pp. 4359–4372, 2011.

[8] A. Leith, M.-S. Alouini, D. I. Kim, X. Shen, and Z. Wu, “Flexible proportional-rate scheduling for OFDMA system,” *IEEE Transactions on Mobile Computing*, vol. 12, no. 10, pp. 1907–1919, 2013.

[9] R. Aggarwal, M. Assaad, C. E. Koksal, and P. Schniter, “Joint scheduling and resource allocation in the OFDMA downlink: Utility maximization under imperfect channel-state information,” *IEEE Transactions on Signal Processing*, vol. 59, no. 11, pp. 5589–5604, 2011.

[10] M. Mehrjoo, S. Moazeni, and X. Shen, “Resource allocation in OFDMA networks based on interior point methods,” *Wireless Communications and Mobile Computing*, vol. 10, no. 11, pp. 1493–1508, 2010.

[11] T. Shi, S. Zhou, and Y. Yao, “Capacity of single carrier systems with frequency-domain equalization,” in *Proc. of IEEE Circuits and Systems Symposium on Emerging Technologies: Frontiers of Mobile and Wireless Communication*, 2004, pp. 429–432.

[12] M. Hua, B. Ren, M. Wang, J. Zou, C. Yang, and T. Liu, “Performance analysis of OFDMA and SC-FDMA multiple access techniques for next generation wireless communications,” in *Proc. of IEEE Vehicular Technology Conference (VTC Spring)*, 2013, pp. 1–4.

[13] T. Liu, C. Yang, and L.-L. Yang, “A low-complexity subcarrier-power allocation scheme for frequency-division multiple-access systems,” *IEEE Transactions on Wireless Communications*, vol. 9, no. 5, pp. 1564–1570, 2010.

[14] W. Dang, M. Tao, H. Mu, and J. Huang, “Subcarrier-pair based resource allocation for cooperative multi-relay OFDM systems,” *IEEE Transactions on Wireless Communications*, vol. 9, no. 5, pp. 1640–1649, 2010.

[15] T. Wang and L. Vandendorpe, “Sum rate maximized resource allocation in multiple DF relays aided OFDM transmission,” *IEEE Journal on Selected Areas in Communications*, vol. 29, no. 8, pp. 1559–1571, 2011.

[16] X. Zhang, X. Shen, and L.-L. Xie, “Joint subcarrier and power allocation for cooperative communications in LTE-Advanced networks,” *IEEE Transactions on Wireless Communications*, vol. 13, no. 2, pp. 658–668, 2014.

[17] M. S. Alam, J. W. Mark, and X. Shen, “Relay selection and resource allocation for multi-user cooperative OFDMA networks,” *IEEE Transactions on Wireless Communications*, vol. 12, no. 5, pp. 2193–2205, 2013.

[18] J. Zhang, L.-L. Yang, and L. Hanzo, “Energy-efficient channel-dependent cooperative relaying for the multiuser SC-FDMA uplink,” *IEEE Transactions on Vehicular Technology*, vol. 60, no. 3, pp. 992–1004, 2011.

[19] ——, “Energy-efficient dynamic resource allocation for opportunistic-relaying-assisted SC-FDMA using turbo-equalizer-aided soft decode-and-forward,” *IEEE Transactions on Vehicular Technology*, vol. 62, no. 1, pp. 235–246, 2013.

[20] A. Lo and P. Guan, “Performance of in-band full-duplex amplify-and-forward and decode-and-forward relays with spatial diversity for next-generation wireless broadband,” in *IEEE ICOIN*, 2011, pp. 290–294.

[21] L.-L. Xie and P. Kumar, “An achievable rate for the multiple-level relay channel,” *IEEE Transactions on Information Theory*, vol. 51, no. 4, pp. 1348 –1358, 2005.

[22] 3GPP. TS 36.211 Technical Specification Group Radio Access Network; Evolved Universal Terrestrial Radio Access (E-UTRA); Physical Channels and Modulation (Release 8).

[23] T. M. Cover and J. A. Thomas, *Elements of information theory*. John Wiley & Sons, 1991.

[24] M. Noune and A. Nix, “Performance of SC-FDMA with transmit power allocation and frequency-domain equalization,” in *Proc. of International Symposium on Personal Indoor and Mobile Radio Communications (PIMRC)*, 2010, pp. 852–857.

[25] M.-L. Ku and H.-J. Yeh, “Channel equalization and chunk assignment schemes for LTE SC-FDMA systems in multipath channels,” in *Proc. of IEEE International Conference on Communication Technology (ICCT)*, 2012, pp. 1166–1171.

[26] 3GPP. TS 36.116 Technical Specification Group Radio Access Network; Evolved Universal Terrestrial Radio Access (E-UTRA); Relay Radio Transmission and Reception (Release 11).

Xiaoxia Zhang received the B.E. degree from Beijing University of Posts and Telecommunications, Beijing, China in 2008 and M.A.Sc. degree in Electrical and Computer Engineering from the University of Waterloo, Waterloo, ON, Canada in 2010. She is currently working towards the Ph.D. degree at the Department of Electrical and Computer Engineering, University of Waterloo, Waterloo, ON, Canada. Her research interests include resource management for broadband communication networks, cooperative communication, wireless sensor networks and network information theory.

This article has been accepted for publication in a future issue of this journal, but has not been fully edited. Content may change prior to final publication. Citation information: DOI 10.1109/TVT.2015.2416714, IEEE Transactions on Vehicular Technology

Xuemin (Sherman) Shen (IEEE M'97-SM'02-F'09) received the B.Sc. (1982) degree from Dalian Maritime University (China) and the M.Sc. (1987) and Ph.D. degrees (1990) from Rutgers University, New Jersey (USA), all in electrical engineering. He is a Professor and University Research Chair, Department of Electrical and Computer Engineering, University of Waterloo, Canada. He was the Associate Chair for Graduate Studies from 2004 to 2008. Dr. Shen's research focuses on resource management in interconnected wireless/wired networks, wireless network security, social networks, smart grid, and vehicular ad hoc and sensor networks. Dr. Shen served as the Technical Program Committee Chair/Co-Chair for IEEE Infocom'04, IEEE VTC'10 Fall, the Symposia Chair for IEEE ICC'10, the Tutorial Chair for IEEE VTC'11 Spring and IEEE ICC'08, the Technical Program Committee Chair for IEEE Globecom'07, the General Co-Chair for Chinacom'07 and QShine'06, the Chair for IEEE Communications Society Technical Committee on Wireless Communications, and P2P Communications and Networking. He also serves/served as the Editor-in-Chief for IEEE Network, Peer-to-Peer Networking and Application, and IET Communications; a Founding Area Editor for IEEE Transactions on Wireless Communications; an Associate Editor for IEEE Transactions on Vehicular Technology, Computer Networks, and ACM/Wireless Networks, etc.; and the Guest Editor for IEEE JSAC, IEEE Wireless Communications, IEEE Communications Magazine, and ACM Mobile Networks and Applications, etc. Dr. Shen received the Excellent Graduate Supervision Award in 2006, and the Outstanding Performance Award in 2004, 2007 and 2010 from the University of Waterloo, the Premier's Research Excellence Award (PREA) in 2003 from the Province of Ontario, Canada, and the Distinguished Performance Award in 2002 and 2007 from the Faculty of Engineering, University of Waterloo. Dr. Shen is a registered Professional Engineer of Ontario, Canada, an IEEE Fellow, an Engineering Institute of Canada Fellow, a Canadian Academy of Engineering Fellow, and a Distinguished Lecturer of IEEE Vehicular Technology Society and Communications Society.

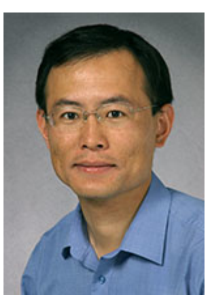

Liang-Liang Xie (IEEE M'03-SM'09) received the B.S. degree in mathematics from Shandong University, Jinan, China, in 1995 and the Ph.D. degree in control theory from the Chinese Academy of Sciences, Beijing, China, in 1999.

He did postdoctoral research with the Automatic Control Group, Linköping University, Linköping, Sweden, during 1999-2000 and with the Coordinated Science Laboratory, University of Illinois at Urbana-Champaign, during 2000-2002. He is currently a Professor at the Department of Electrical and Computer Engineering, University of Waterloo, Waterloo, ON, Canada. His research interests include wireless networks, information theory, adaptive control, and system identification.